The duration of load effect in lumber as stochastic degradation

Samuel W. K. Wong* and James V. Zidek†

January 6, 2019

Index terms – gamma process; degradation; duration of load; wood products; accumulated damage models

Abstract

This paper proposes a Bayesian framework for applying a gamma process model for reliability analysis in structural engineering under time–varying stochastic loads. We focus on an important application to engineered wood products and thereby demonstrate how the proposed methodology can be implemented in practice. We use a gamma process to characterize the degradation over time in each piece of lumber, allowing for variability between pieces when external forces from loads are applied to a population of lumber. We propose a model for the shape parameter to accommodate time–varying loads. Our approach is compared with traditional accumulated damage models. Our statistical analysis of experimental data highlight the limitations of using accelerated testing to assess long–term reliability, as seen in the wide posterior intervals. This suggests the need for more comprehensive testing in future applications, or to encode appropriate expert knowledge in the priors used for Bayesian analysis.

*Department of Statistics and Actuarial Science, University of Waterloo, Waterloo, ON, Canada. E-mail: samuel.wong@uwaterloo.ca

†Department of Statistics, University of British Columbia, Vancouver, BC, Canada. E-mail: jim@stat.ubc.ca

Abbreviations and acronyms
ADM: accumulated damage model
DOL: duration of load
ODE: ordinary differential equation
psi: pounds per square inch
MCMC: Markov Chain Monte Carlo
CDF: cumulative distribution function

Notation
$\alpha(t)$: damage accumulated at time t
$\sigma(t)$: stress ratio at time t
$\tau(t)$: load applied at time t
τ_s: short-term strength
σ_0: ADM stress ratio threshold
Y_t: degradation stochastic process
T: failure time
f_T: probability density of failure time
τ_i: a load level threshold
$\tilde{t}_i$: total time duration that load exceeded τ_i
η_t: Gamma process shape parameter
ξ: Gamma process scale parameter
τ^*: population stress threshold
θ: vector of model parameters
$\pi(\theta)$: prior distribution of model parameters
$\theta^{(1)}, \theta^{(2)}, \ldots, \theta^{(N)}$: MCMC samples of parameters

1 Introduction

Wood placed under a sustained load over a period of time in an engineering application will sustain damage due to the "duration of load" (DOL) effect [1]. The importance of this effect led to the development of models for predicting it so that it could be incorporated into the establishment of design values and safety factors in applications. However shortcomings in these models that we now describe led to the development by the authors of the alternative approach described in this paper. The two approaches are then compared in an illustrative application.

Long term damage in a piece of lumber, resulting in a reduction of its strength-bearing capacity, depends on the load level and how it is applied (e.g., via bending, compression, tension). The speed at which a piece weakens over time may also depend on a combination of factors such as the visco–elasticity of the wood, temperature and moisture. Even a relatively small constant load applied over a sufficiently long period of time may lead to failure (known as creep rupture). According to the review of Rosowsky and Bulleit [2], the effect was first recognized by Haupt [3]. But it does not seem to have been formally incorporated into design standards until Wood et al. [4] produced the so–called Madison Curve for doing so. The curve is still in use today for estimating the DOL effect on the strength of wood.

However the purely empirical approach of Wood led only to a fitted curve. So an alternative dynamic model was developed to describe how damage accumulated over time as a function of the stress load profile [5, 6, 7]. These accumulated damage models (ADMs) differ in detail, but the idea is the same. At time t, let $\alpha(t)$ denote the accumulated damage and $\sigma(t)$ denote the so-called stress ratio. Then ADMs focus on the rate at which damage accumulates rather than the damage itself, using an ordinary differential equation (ODE)

$$\frac{d\alpha(t)}{dt} = F[\alpha(t), \sigma(t), \phi], \tag{1}$$

which represents the rate of damage accumulation for a randomly selected piece of lumber. The vector ϕ contains (random) parameters associated with the piece itself, with their joint probability distribution depending on population parameters that must also be fitted to implement the model. Once a piece is selected, the model (1) deterministically describes the rate at which damage accumulates in that piece.

While $\alpha(t)$ is unobservable, the ODE provides a framework onto which the other elements of the model can be attached. It is calibrated so that $\alpha(t) = 0$ when $t = 0$ and no damage has occurred, and $\alpha(T_l) = 1$ at time $t = T_l$ when the piece fails. The stress ratio is defined as $\sigma(t) = \tau(t)/\tau_s$, where $\tau(t)$ (psi) is the applied stress at time t and τ_s (psi) is the 'short-term

breaking strength' of the piece (commonly defined to be the stress at which the piece would fail were it to be subjected to a ramp load test of duration ∼1 minute).

For definiteness, this paper will focus on a representative and well–known ADM, the "Canadian model" proposed by [8]. That model is based on the two-term approximation obtained from a Taylor expansion of F in Equation (1) as a function of $\alpha(t)$, namely

$$\dot{\alpha}(t) = a[\tau(t) - \sigma_0\tau_s]_+^b + c[\tau(t) - \sigma_0\tau_s]_+^n \alpha(t) \tag{2}$$

where b, c, n, σ_0, τ_s are log–normally distributed random effects for the piece, and a is determined as a function of those five random effects. Here σ_0 is known as the stress ratio threshold, and $x_+ = \max(x, 0)$. Thus in this model, no damage accumulates in the piece when $\tau(t) < \sigma_0\tau_s$.

However Ellingwood and Rosowsky [9] point out that the Canadian model cannot be nondimensionalized. That is a serious issue, since a model that represents a natural process cannot ultimately depend on how the quantities involved in the model are measured. The concern was seen to be of sufficient importance that Ellingwood and Rosowsky [9] exclude the model from their comparative analysis of ADMs. The review of ADMs in Hoffmeyer and Sørensen [10] instead modifies the Canadian model to correct the dimensions; this difficulty of the Canadian model, as well as in other ADMs, was also described in Zhai [11] and Zhai et al. [12]. Wong and Zidek [13] also address the problem by invoking the Buckingham π theorem to build reparametrized models that are dimensionally consistent while retaining their functional form.

Another difficulty associated with the ADM approach is its computational burden due to the need to solve ODEs such as Equation (2) numerically for each individual piece of lumber, one that restricts the use of standard likelihood-based methods for their analysis. As a result, uncertainties in both the parameter estimates and subsequent reliability calculations are difficult to quantify. Yang et al. [14] address this latter difficulty by proposing approximate Bayesian computation techniques to perform the analysis on a solid statistical platform; however, a large cluster of CPUs is needed to carry out the subsequent reliability calculations with high–accuracy ODE numerical solvers.

As a final limitation of the ADM approach, randomness in the process of damage accumulation within a given piece is ignored, which may not be realistic. In consequence, estimates of ADM parameters are difficult to interpret as population level and piece–specific modeling are inherently intertwined. So this paper studies the use of a gamma process, as an alternative for modelling the DOL effect that overcomes the difficulties described above.

The gamma process has a long history as an approach for modelling degradation [15]

and determining the need for maintenance from degradation data obtained from routine inspections [16]. By specifying an appropriate functional form for its shape parameter, the gamma process also has the flexibility to be used for studying time-dependent reliability of structures [17, 18]. This leads us to a key contribution of this paper: motivated by the lumber application, in this paper we develop a specific functional form for the shape parameter to study the DOL effect under a time-varying load. The proposed form for the model is expected to be broadly applicable to future study of other materials susceptible to a similar DOL effect, such as oriented strand board [19].

In a major point of departure from the ADM approach above, the degradation of a piece of lumber under the gamma process remains random (even conditional on it having being selected): it is represented by a stochastic process $Y_t,\ t \geq 0$, that describes the damage accumulated up to time t. That process is internal to the piece, and can be thought of as representing its random progress of damage. The future combination of dead and live loads, which may be a random process, are external to that piece. Given a realized load profile, these two ingredients are fused through the deterministic time–varying population level shape parameter. This separation of internal and external sources of variability has advantages in terms of the interpretability of the results and facilitates the use of principled statistical methods of analysis.

Specifically, we present Bayesian methods for fitting the gamma process model to data obtained in an accelerated testing experiment designed to explore the duration of load effect. Adopting a Bayesian approach for inference here has two appealing features. First, it permits *a priori* knowledge about any of the model parameters, when available, to be incorporated in the priors for analysis. Second, the Bayesian framework allows uncertainty in the model parameters to be coherently accounted for, in subsequent posterior predictions such as reliability estimates.

The paper is organized as follows. Section 2 introduces the gamma process as a way of describing the damage due to the stress applied to wood when placed in service. Section 3 describes how the gamma process may be used to characterize degradation, and develops a model for the time-varying shape parameter motivated by the lumber application. Bayesian methods for analysis and their use on an illustrative dataset are presented in Section 4. The fitted model is applied to reliability analysis in Section 5. Another application follows in Section 6; there it is shown how the residual life of a piece of lumber in service can be predicted. Further discussion and concluding remarks follow in Section 7.

2 The gamma process as a specimen–specific stochastic model

In this section we briefly review the basics of the gamma process as it relates to modeling lumber degradation.

Let $Y_t \geq 0$ be the stochastic process representing the accumulated damage (or degradation in the terminology of reliability theory) in a piece of lumber at time t. Assume $Y_0 = 0$ and that $Y_t \geq 0$ is nondecreasing over time, as any damage sustained is irreversible. We say that the piece reaches a state of failure at time $t = T$ when the damage exceeds a pre-specified threshold level indicating failure. Without loss of generality, we may scale the degradation process so that failure occurs at $Y_T = 1$. Virtually, the degradation process can be thought to continue for $t > T$ even though by that time the specimen will have failed.

Conditional on the parameters for a randomly selected lumber specimen, assume $Y_t,\ t \geq 0$ has stochastically independent increments, i.e. for any sequence of times $t_1 < \cdots < t_n$, the increments $Y_{t_i} - Y_{t_{i-1}},\ i = 1, \ldots n$ are stochastically independent. The distribution of these increments may depend on factors internal to the specimen as well as the external effects of the applied stress, resulting in damage that accumulates as a series of successive jumps of random size. The particularly simple family of models we adopt assumes Y_t is a compound Poisson process with intensity function $\lambda_t,\ t > 0$, i.e.

$$Y_{t_i} - Y_{t_{i-1}} = \sum_{j=N(t_{i-1})+1}^{N(t_i)} X_j$$

where $N(t)$ is the conventional counting process associated with the Poisson process with $N_{(t_{i-1},t_i)} = N(t_i) - N(t_{i-1})$, and conditional on the model parameters

$$\begin{aligned} P[N_{(t_{i-1},t_i)} = n] &= \frac{\Lambda^n_{(t_{i-1},t_i)} \exp\{-\Lambda_{(t_{i-1},t_i)}\}}{n!}, \text{ with} \\ \Lambda_{(t_{i-1},t_i)} &= \int_{t_{i-1}}^{t_i} \lambda_t dt \end{aligned}$$

while the random jumps X_j, which are independent of the Poisson count process, have a gamma distribution with shape parameter η and scale ξ. Standard theory then implies that

conditional on the model parameters

$$\begin{aligned} E[Y_{t_i} - Y_{t_{i-1}}] &= \xi\eta\Lambda_{(t_{i-1},t_i)}, \text{ while} \\ Var[Y_{t_i} - Y_{t_{i-1}}] &= \xi^2\eta(\eta+1)\Lambda_{(t_{i-1},t_i)}. \end{aligned}$$

As the intensity parameter increases and the gamma shape parameter decreases, we approach in the limit, the so–called gamma process that has an infinite number of infinitesimally small jumps and a time-dependent shape parameter η_t. That model has been used extensively to model degradation. More formally

$$Y_{t_i} - Y_{t_{i-1}} \sim Ga[\xi, \eta_{t_i} - \eta_{t_{i-1}}]$$

where $\eta_t \geq 0$ is a nondecreasing function over time, and $Ga[\xi, \eta_t]$ denotes the gamma distribution with scale parameter ξ and shape parameter η_t. The scale $\xi = \xi(x)$ is a scalar-valued quantity that could also depend on fixed covariates x associated with a specimen, such as the modulus of elasticity. From standard theory we then obtain the mean, variance, and coefficient of variation as

$$\begin{aligned} E[Y_t \mid \xi, \eta_t] &= \xi(x)\eta_t \\ Var[Y_t \mid \xi, \eta_t] &= \xi(x)^2\eta_t \\ CV[Y_t \mid \xi, \eta_t] &= \eta_t^{-1/2}. \end{aligned}$$

Provided that multiple gamma processes have the same scale ξ, which in effect means each has a scale that is a known multiple of ξ, their sum is also a gamma process. More precisely, assume that conditional on η_{it} and ξ, the $\{Y_{it}\}$, $i = 1, \ldots r$ are independent gamma processes with shapes η_{it} and scales ξ. Then the sum

$$Y_t = Y_{1t} + \cdots + \ldots Y_{rt} \tag{3}$$

is also a gamma process with shape $\eta_t = \sum_i \eta_{it}$ and scale ξ.

This is a useful property since it provides a convenient framework for combining different processes that contribute to degradation. The process corresponding to damage due to the applied load profile is that of primary interest in this paper. As potential extensions, other external factors that contribute to damage such as the time-varying moisture content and temperature of the environment could be incorporated as separate components in Equation (3). However, we do not at present have the data to illustrate these refinements to the model.

3 Degradation to failure

3.1 Probability distribution of failure time

The gamma process induces a probability distribution of failure time T, which we briefly review as follows. Detailed proofs of these results can be found in Paroissin and Salami [20]. The survival function for T is

$$P[T > t \mid \xi, \eta_t] = P[Y_t \leq 1 \mid \xi, \eta_t] = \int_0^1 \frac{u^{\eta_t - 1} e^{-u/\xi}}{\xi^{\eta_t} \Gamma[\eta_t]}\, du = 1 - \frac{\Gamma(\eta_t, 1/\xi)}{\Gamma(\eta_t)}, \tag{4}$$

where $\Gamma(\cdot, \cdot)$ denotes the upper incomplete gamma function. When η_t is differentiable, it follows that the probability density of T needed for the construction of the likelihood function is

$$\begin{aligned} f_T[t \mid \xi, \eta_t] &= -\frac{dP[T > t \mid \xi, \eta_t]}{dt} \\ &= \dot{\eta}_t \left(\Psi(\eta_t) - \log(1/\xi)\right) \left(1 - \frac{\Gamma(\eta_t, 1/\xi)}{\Gamma(\eta_t)}\right) \\ &\quad + \frac{\dot{\eta}_t}{\eta_t^2 \Gamma(\eta_t)} (1/\xi)^{\eta_t}\, {}_2F_2(\eta_t, \eta_t; \eta_t + 1, \eta_t + 1; -1/\xi), \end{aligned} \tag{5}$$

where Ψ is the digamma function and ${}_pF_q$ is the generalized hypergeometric function of order p, q.

3.2 Damage due to load applied

Of primary interest is characterizing the gamma process representing damage due to the stress applied. Suppose the load profile over time with which the population is stressed, $\tau(t); t \geq 0$ is given. Then $\tau(t)$ has a fundamental role in determining the corresponding value of η_t. In particular, η_t must account for the degradation effects of the entire load history profile until time t. For lumber degradation, we assume two basic properties for η_t:

(i) If $\tau(t) \leq \tau^*$ for $\delta_1 \leq t \leq \delta_2$, then $\dot{\eta}_t = 0 \ \ \forall \ \ t \in (\delta_1, \delta_2)$, where τ^* is a threshold stress level below which the population does not undergo degradation.

(ii) If $\tau(t)$ is held at a constant level larger than τ^* for $\delta_1 \leq t \leq \delta_2$, then $\dot{\eta}_t$ is decreasing over the interval $\delta_1 \leq t \leq \delta_2$.

The first property implies that degradation does not progress during periods when the stress is too low to cause damage. The threshold τ^* is a population analogue of the damage threshold commonly seen in ADMs (see Introduction). The second property captures the

DOL effect: if the load is held constant at a stress level high enough to cause failures in the population, degradation continues as that constant load is maintained but the rate at which it occurs is expected to slow over time. These properties will guide the specific choice of η_t.

3.3 A model for the shape parameter

We now develop a specific functional form for the shape parameter η_t along with parameters to be estimated from data in the illustrative example. The "power law" and its variants have been commonly used to model degradation and serves as a useful starting point for developing specific model implementations.

For conceptual development, first suppose τ is a given load level held constant over time. Then we can conceive a simple form for η_t to characterize the degradation in a population of pieces subject to that load from time 0 to t as

$$\eta_t = g(t) \times u(\tau - \tau^*)_+, \tag{6}$$

where $g(\cdot)$ is an increasing function that captures the DOL effect, u and τ^* are positive constants, and $x_+ = \max(x, 0)$. Here the term $u(\tau - \tau^*)_+$ is constant over time, depending only on the size of the load. It is zero when that stress level is sufficiently low in accord with property (i), that is when $\tau < \tau^*$, where τ^* is the stress threshold below which no degradation occurs. The function $g(t)$ governs the rate of degradation in the population over time under that fixed load. The simple form $g(t) = t^a$ with $a > 0$ would reproduce the well-known power law. Various modifications can be made to increase its flexibility to model the degradation behaviour, and we will perform our subsequent analysis using the form $g(t) = t^a + bt^c$ where a, b, c are all positive parameters with $a < c$, which has the feature of mixing two different power law growth rates and satisfies the differentiability requirement of η_t in Equation (5). In particular, setting the constraint $a < c$ ensures a unique curve for $g(t)$ where t^a has the more important role in describing shorter-term effects, while the role of bt^c becomes more important over longer time durations. The parameters a, b, c are identifiable under this constraint: two different sets of parameters a_1, b_1, c_1 and a_2, b_2, c_2 cannot yield the same function for all $t > 0$, namely $t^{a_1} + b_1 t^{c_1} = t^{a_2} + b_2 t^{c_2}$ implies $a_1 = a_2, b_1 = b_2, c_1 = c_2$.

In practice, the load may vary over time and so we now generalize the reasoning above to handle an arbitrary load profile $\tau(t)$. Let $0 = \tau_0 < \tau_1 < \tau_2 < \cdots < \tau_m$ denote a sequence of load levels spanning the range of loads under which the population may be subjected. Then for each load level τ_i, $i = 1, \ldots, m$, we can consider the amount of incremental degradation due to load τ_i beyond that which was sustained from load τ_{i-1}. Then a natural analogue to

Equation (6) for this load increment, for time 0 to t, is

$$g(\tilde{t_i})\left[u(\tau_i - \tau^*)_+ - u(\tau_{i-1} - \tau^*)_+\right],$$

where $\tilde{t_i} = \int_0^t I(\tau(t') \geq \tau_i)\, dt'$ is the total time duration for which the load exceeded τ_i. Thus the constant term $[u(\tau_i - \tau^*)_+ - u(\tau_{i-1} - \tau^*)_+]$ captures the incremental 'jump' in η_t that occurs due to load level τ_i being reached. The size of the 'jump' depends on the difference $\tau_i - \tau_{i-1}$; for example, if we were to set $\tau_i = \tau_{i-1}$ then the proposed expression for the load increment is zero as should be expected. Similarly $g(\tilde{t_i})$, as a function of the total length of time for which the load level τ_i is sustained, now models its corresponding DOL effect.

We can then combine the contributions of all the load levels to construct η_t for any arbitrary given load profile. Using our chosen form for $g(t)$, we thus obtain

$$\eta_t = \sum_{i=1}^{m} (\tilde{t_i}^a + b\tilde{t_i}^c)\left[u(\tau_i - \tau^*)_+ - u(\tau_{i-1} - \tau^*)_+\right]. \tag{7}$$

This expression can coherently simplify to Equation (6) in the special case that the load is held constant at τ from time 0 to t, since by setting $\tau_m = \tau$ we will have $\tilde{t_i} = t$ for all $i = 1, \ldots, m$. Further, it can be seen that η_t is differentiable, since if $\tau_j \leq \tau(t) < \tau_{j+1}$, we have

$$\dot{\eta}_t = \sum_{i=1}^{j} (a\tilde{t_i}^{a-1} + bc\tilde{t_i}^{c-1})\left[u(\tau_i - \tau^*)_+ - u(\tau_{i-1} - \tau^*)_+\right] \tag{8}$$

using the fact that $d\tilde{t_i}/dt = I(\tau(t) \geq \tau_i)$. That is, at time t only the load thresholds below $\tau(t)$, namely $\tau_1, \ldots, \tau_j$, contribute to the rate of increase in the shape parameter. Also, it can be seen that when the exponents a and c are each less than 1, $\dot{\eta}_t$ is decreasing over any period with a fixed load level, in accord with property (ii).

A specific sequence of load levels $\tau_1, \ldots, \tau_m$ needs to be chosen for computation. These serve as the incremental thresholds over which additional degradation contributions are added into the model. For example, if $\tau_j = 3000$psi and $\tau_{j+1} = 3020$psi, then any loads in the interval $[3000, 3020)$ would contribute the same amount to η_t in this model as a load of exactly 3000psi. Naturally, the range of loads may be discretized as finely as desired to faithfully reproduce the stress history, at the cost of additional computation time. In our demonstration we use an equally-spaced sequence for $\tau_1, \ldots, \tau_m$ with intervals of 20psi. An artifact of the discrete load levels in the model is that if the load profile $\tau(t)$ has periods of continuous increase, the resulting η_t becomes jagged as the load passes the different thresholds rather than smoothly increasing with the load. In this case a line segment can be used

to smooth η_t between the time points when successive load thresholds are reached, to serve as an acceptable approximation.

4 A Bayesian analysis of degradation

This section presents a Bayesian analysis of data from an accelerated testing experiment designed to explore the duration of load effect.

4.1 The data

The real data we subsequently analyze come from the DOL experiment reported in Foschi and Barrett [21]. It consists of a total of 637 pieces of visually graded 2x6 Western Hemlock, divided for testing under three different load profiles, as listed below. All time units are hours unless otherwise indicated, and the loading rate of 388440psi/hour is the rate used for calibrating the short-term strength of lumber of this size in ASTM Standard D 4761-88 [22].

1. 198 pieces were assigned the load profile

$$\tau(t) = \begin{cases} 388440t, & \text{for } t \leq 3000/388440 \\ 3000, & \text{for } 3000/388440 < t \leq 4 \text{ years}, \end{cases}$$

   i.e., the load was increased linearly until reaching 3000psi, and held at that constant level for 4 years. Hence pieces that do not fail by the end of the 4-year period when the test is truncated have their failure time censored.

2. 300 pieces were assigned the load profile

$$\tau(t) = \begin{cases} 388440t, & \text{for } t \leq 4500/388440 \\ 4500, & \text{for } 4500/388440 < t \leq 1 \text{ year}, \end{cases}$$

   which is similar to the above, now with a constant load level of 4500psi for 1 year. Pieces that do not fail by the end of the 1-year period when the test is truncated have their failure time censored.

3. 139 pieces were assigned the load profile $\tau(t) = 388440t$ until failure.

In the DOL literature, profiles 1 and 2 are known as 'constant load' tests, while profile 3 is known as a 'ramp load' test. These are so-called 'accelerated' testing schemes that were originally designed to help elucidate the long-term DOL effect using tests of relatively shorter

duration [6]. DOL models fitted to these data are then applied in reliability analyses with arbitrary load profiles.

Each piece that failed during the test had its failure time recorded. Pieces that did not fail during the test duration had their censoring times recorded (i.e., 4 years for group 1 and 1 year for group 2). No covariates for individual specimens were recorded in the data.

4.2 Model fitting procedure

We now describe how to fit the model to these accelerated testing data, using the techniques of Bayesian inference. Let θ denote the vector of parameters to be inferred, which consists of the five parameters associated with the model for η_t along with the gamma process scale parameter ξ, namely $\theta = (a, b, c, u, \tau^*, \xi)$. Let $\pi(\theta)$ denote the joint prior distribution on θ which encodes any prior knowledge on θ. The likelihood of the observed failure time of an individual specimen is given by Equation (5). Then, the form of the posterior distribution for θ, based on an independent sample of test specimens with recorded failure times $t_1, t_2, \ldots, t_n$, is given by the product of the prior and the likelihood of the sample,

$$\pi(\theta|t_1, t_2, \ldots, t_n) \propto \pi(\theta) \prod_{i=1}^{n} f_T(t_i|\xi, \eta_{t_i}), \tag{9}$$

where η_{t_i} denotes evaluating Equation (7) for η_t at time t_i according to the load profile $\tau(t)$ associated with specimen i. For some specimens the actual failure times are not observed, as the test has ended after a specified duration without the specimen failing. Then the likelihood contribution $f_T(t_i|\xi, \eta_{t_i})$ for each of those specimens is replaced by the corresponding survivor function, namely $P(T_i > t_c|\xi, \eta_{t_i})$ computed by Equation (4) where t_c is the truncation time.

Equation (9) thus can accommodate all the test data to be analyzed under the different loading profiles employed in the experiment. Importantly, we emphasize it is assumed that the same set of parameters can model the degradation of the population under *any* loading scenario. That assumption, which implies that the parameters of a fitted model can then be used with any load profile $\tau(t)$ of interest, has been fundamental to much of the previous work with ADMs that involve the probabilistic assessment of long-term lumber reliability. An example of such follows in Section 5.

The joint posterior distribution of θ, namely $\pi(\theta|t_1, t_2, \ldots, t_n)$ given in Equation (9), is the basis for inference on the parameters. We may represent that posterior distribution by drawing a large number of random samples from it. It can be seen from the expressions in Equations (5) and (7) that the posterior has a nonstandard distribution for any choice of prior, and intractable for directly drawing random samples from it. We thus employ standard

Markov Chain Monte Carlo (MCMC) techniques to obtain sample draws. First, to obtain reasonable starting values of θ for the MCMC, we use the Nelder–Mead method to optimize the posterior as a function of θ. Second, we use the Metropolis-Hastings algorithm [23] with a Normal random-walk proposal to update the six parameters of θ at each MCMC iteration, where the proposal scale may be tuned to achieve a reasonable acceptance rate between 20-50%. Standard MCMC theory guarantees convergence to the posterior distribution, as shown in p.113-115 of [24]. As there are just six parameters, it is more efficient here to update all parameters simultaneously at each iteration compared to updating one at a time via Gibbs sampling. Third, we use multiple MCMC chains to improve mixing and increase the efficiency of posterior exploration, by employing parallel tempering [25] with geometrically spaced temperatures and distributed over multiple CPU cores. After discarding an appropriate burn-in period, the remaining iterations of the MCMC chain representing the target posterior distribution are the samples of θ used for inference.

4.3 Model fitting results

To proceed with our illustrative analysis, we complete the specification of the posterior in Equation (9) by choosing prior $\pi(\theta)$. Without specific *a priori* knowledge, we opt to use flat independent Uniform$[0, 10000]$ priors for each of the parameters in θ with the restriction that $a < c$, that is, samples that fail to meet this constraint in MCMC are rejected.

First, Nelder–Mead optimization on the posterior distribution yielded the following values of θ which were used as starting values for the MCMC: $(0.0202, 0.0026, 0.26, 0.00085, 659, 0.23)$. Second, the scale used for the Normal Metropolis-Hastings random-walk proposals was a 0.01 factor times the starting values. Third, the parallel tempering scheme was distributed over a cluster of 120 CPU cores with temperatures geometrically spaced from 1 to 20. Swaps between chains were performed after every five Metropolis-Hastings updates. The first 5,000 such iterations were examined and discarded as an appropriate burn-in. The samples from the remaining $N = 15,000$ iterations, which we shall denote as $\theta^{(1)}, \theta^{(2)}, \ldots, \theta^{(N)}$, are used for the inferences that follow.

We summarize the posterior distributions of the parameters in Table 1, by presenting the posterior mean, median, and the central 95% credible interval for each parameter. A few observations can be noted. First, there is a clear distinction between powers a and c, with posterior means of 0.019 and 0.40 respectively, indicating that a single power law does not adequately explain the observed degradation over time. Second, there is only weak evidence for a stress threshold τ^* below which no population degradation occurs; the MCMC samples yield a posterior mean for the threshold level of 413psi and a highly uncertain 95% posterior

interval $(43, 642)$ so that a very low threshold is plausible. Third, the highest uncertainty is in the parameter b, whose central 95% posterior probability interval spans two orders of magnitude: $(0.000071, 0.03732)$. This indicates that the true degradation behaviour over longer time durations (i.e., several years or more) is highly uncertain from these data alone, with the two constant load tests having been truncated at 1 and 4 years.

Table 1: Summary of the posterior distributions of the parameters in the fitted gamma process model: posterior means, medians, and central 95% credible intervals.

Parameter	Mean	Median	95% interval
a	0.019	0.019	(0.012, 0.027)
b	0.01026	0.00729	(0.00071, 0.03732)
c	0.40	0.39	(0.25, 0.60)
u	0.00088	0.00088	(0.00071,0.00108)
τ^*	413	447	(43, 642)
ξ	0.21	0.21	(0.16, 0.26)

The fits of the proposed model for the data from the three test scenarios are visualized on the plots shown in Figure 1. For each posterior draw $\theta^{(1)}, \theta^{(2)}, \ldots, \theta^{(N)}$, a corresponding cumulative distribution function (CDF) is computed from Equation (4). The 0.025 and 0.975 quantiles of these at each time point are used as the lower and upper limits of the 95% posterior bands shown in grey. The dashed curve is the CDF corresponding to the sampled parameter vector with the highest posterior density. Beyond the test truncation times, namely 4 years for the 3000psi constant load group and 1 year for the 4500psi constant load group, the uncertainty increases substantively as seen in the width of the posterior intervals. Hence projections of degradation over the long term, say 30 or 50 years, based on these data alone would likewise have very high variability.

Next, we compare our fitted model to the Canadian ADM in Equation (2). Estimates for the 10 parameters of the Canadian ADM, fitted to the same dataset using a non-linear least squares method, are provided in Tables 1 and 2 of [26]. As mentioned in the Introduction, the ADM approach does not yield an analytically tractable likelihood function; however, we can obtain a good numerical approximation of the likelihood following the techniques described in [14]. Briefly, we simulate 100,000 realizations of the random effects in Equation (2) according to the log-normal parameters; then, we solve the ODE Equation (2) for each realization to obtain failure times under the different loading scenarios. A kernel density smoother is then applied to the empirical distribution of failure times to estimate the probability density for the likelihood computation; the large number of realizations used (100,000) ensures a stable density estimate. Following this procedure, the log-likelihood of the data under the Canadian model is computed to be -640.8. In contrast, the θ with the highest log-likelihood

value among our MCMC samples is -631.3. The log-likelihood values allow us to compute the Bayesian Information Criterion (BIC) [27], which is widely-used for comparing models. The BIC for the Canadian model with 10 parameters is 1346.2, and that of our gamma process model with six parameters is significantly lower at 1301.4; this presents strong evidence that our model is overall a better fit to the same data.

The fit of the data to the Canadian model can be seen in Figure 3 of [26]; here we briefly comment on the visual aspects of the two model fits. Our gamma process model fits the ramp load data well, but tends to overestimate and underestimate the CDF over a broad range in the 3000psi and 4500psi constant-load scenarios respectively. In contrast, the CDFs based on the Canadian model fit the empirical CDFs better for those ranges of the constant-load scenarios. By examining the lower tails of the three distributions, the respective deficiencies of the two models for fitting this particular datset become apparent. The Canadian model fits the shortest failure times poorly in all three scenarios, and the underestimated probability density leads to poor likelihood values for the data in those ranges. The gamma process model, in contrast, fits the lower tails well but does not correctly calibrate the probability density near the transition point from ramp to constant load.

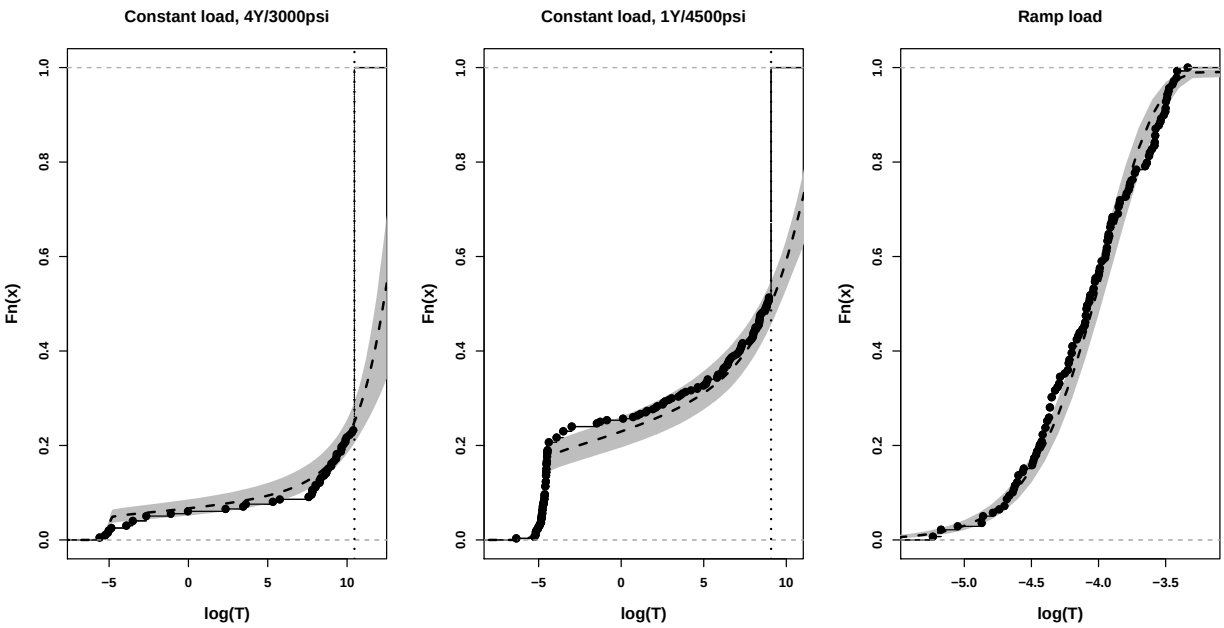

Figure 1: Cumulative distribution functions (CDFs) associated with the fitted gamma process model, on the three calibration datasets. In each plot, the black points show the empirical CDF of the dataset. The dashed curve is the CDF associated with the set of parameters with the highest posterior density among the MCMC samples, while the grey area represents the 95% posterior probability interval of the CDF based on the MCMC samples. The vertical dotted lines indicate the censoring times for the two constant load scenarios.

5 Reliability analysis: an illustrative example

We now turn to applying the fitted model to an example of a predictive scenario, such as those analyzed in reliability assessments. Foschi et al. [28] use stochastic processes to characterize load profiles on individual lumber members over the lifetime of a wood structure, and an adapted example of a heavier than typical 50-year load profile for a residential dwelling unit is shown in the left panel of Figure 2. This profile is a piecewise constant function obtained by summing different component loads. Intuitively, the total load at any given time includes the constant dead weight of the structure, along with load from occupancy which varies by resident. In addition, the 'spikes' correspond to various short-term loads that are expected to occur periodically in homes.

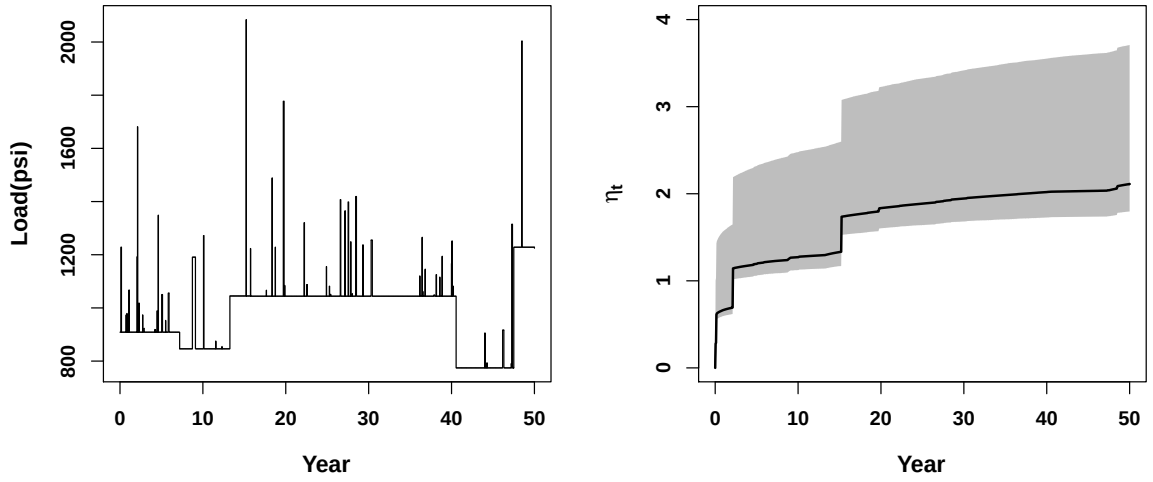

Figure 2: Reliability assessment example. The left panel shows an example of a simulated residential 50-year load profile, adapted from Foschi et al. [28]. The right panel shows the corresponding η_t of the fitted gamma process model under this load profile. The black curve shown is computed on the set of parameters with the highest posterior density among the MCMC samples, while the grey area represents the 95% posterior probability interval based on the MCMC samples.

For a given parameter vector θ and the $\tau(t)$ in the left panel of Figure 2, it is straightforward to compute the corresponding η_t for $t = 0$ to 50 years by plugging into Equation (7). We do this for each of the parameter vectors $\theta^{(1)}, \theta^{(2)}, \ldots, \theta^{(N)}$ sampled by MCMC from the posterior distribution of the parameters in Section 4.3. The solid black curve shows η_t computed for this 50-year period from the sampled parameter vector with the highest posterior density. It can be seen that η_t increases rapidly the first time the load exceeds a new threshold, for example, at time $\sim$2 years (load $\sim$1675psi) and $\sim$15 years (load $\sim$2050psi).

Subsequent loadings translate to more modest degradation increases over time, as expected from the DOL effect; for example, the second time the load exceeds 2000psi at time ∼48 years its effect on η_t is much more diminished. After computing η_t for each of the MCMC samples, the 0.025 and 0.975 quantiles at each time point are used as the lower and upper limits of the 95% posterior bands shown in grey.

Ultimately the probability of failure by the end of the 50-year period is of primary interest. From Equation (4), this probability is given by $\Gamma(\eta_t, 1/\xi)/\Gamma(\eta_t)$ at $t = 50$ years. Evaluating this for each of $\theta^{(1)}, \theta^{(2)}, \ldots, \theta^{(N)}$, the estimated posterior mean for the probability of failure is 0.090 and a central 95% posterior interval is given by $(0.055, 0.150)$. Thus it can be seen that the reliability calculations based on a Bayesian analysis of the gamma process model are fast and simple, and readily provide posterior credible intervals to capture uncertainty.

To compare results, we also take the approach of Foschi et al. [28] based on the Canadian ADM and their parameter estimates for these same data. Here, the probability of failure must be estimated via simulation. We obtain 100,000 simulated failure times by numerically solving the ODE Equation (2) using random b, c, n, σ_0, τ_s drawn from their random effects distributions. The estimated 50-year failure probability is the fraction of simulated specimens that fail by 50 years; for the same load profile in the left panel of Figure 2 the estimate obtained is 0.015. It is not possible to construct a confidence interval on this estimate, as the previous model and estimation approach does not provide confidence intervals on the parameter estimates. Nonetheless, it can be noted that the ADM approach yields a much lower failure probability than that obtained from our gamma process model and falls outside our 95% posterior interval. This comparison is shown visually in Figure 3, where the cumulative failures over 50 years are plotted. The empirical CDF of simulated failure times from the ADM is shown with the black points, while the corresponding CDF computed from the highest posterior density gamma process parameters is shown with the solid black curve with posterior uncertainty in grey.

6 Predicting the residual life of lumber in service

As a further application of the fitted Bayesian model, we may use the MCMC samples from Section 4.3 to compute the posterior probability distributions of the residual life for pieces that have not failed up to a given time t'. Suppose we are given a parameter vector θ, the load history $\tau(t); 0 \leq t \leq t'$, and a characterization of the future load profile $\tau(t); t > t'$. Then we may compute η_t for all $t > 0$ using Equation (7). Let T be the random variable that denotes the failure time of a specimen, then of interest is the distribution of $T_r := [T|T > t'] - t'$

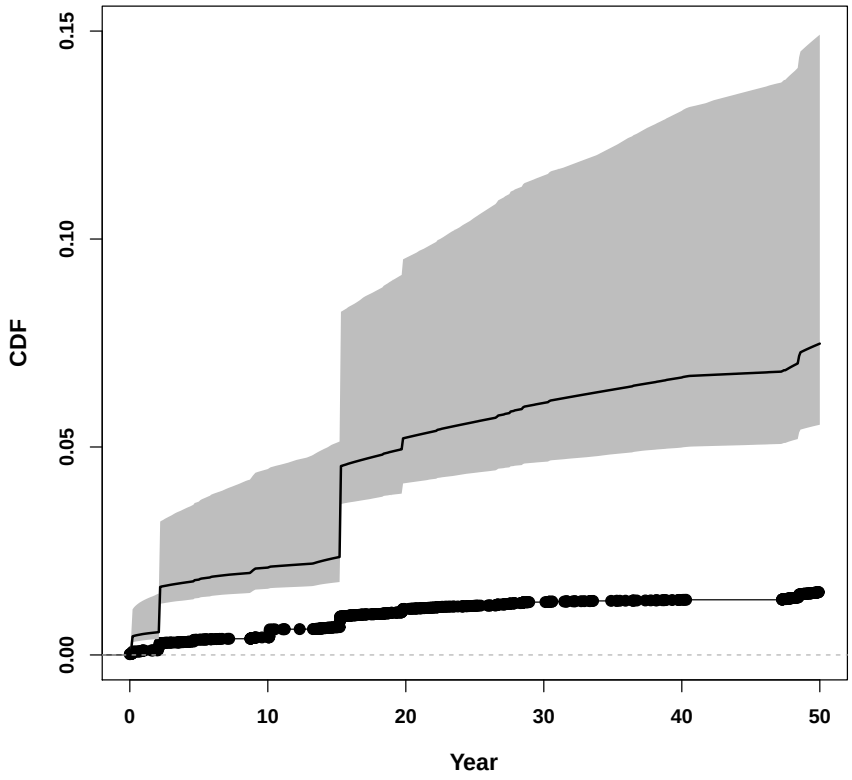

Figure 3: Comparison of 50-year reliability under our Gamma process approach and traditional ADM for the load profile in Figure 2, illustrated via cumulative failure probability. The empirical CDF of simulated failure times from the ADM is shown with the black points. The black curve shown is computed on the set of gamma process parameters with the highest posterior density among the MCMC samples, while the grey area represents the 95% posterior probability interval based on the MCMC samples.

which represents the remaining lifetime. It has survivor function

$$P[T_r > t_r \mid \xi, \eta_t] \;=\; \frac{P[T > t' + t_r \mid \xi, \eta_t]}{P[T > t' \mid \xi, \eta_{t'}]}, \tag{10}$$

where both the numerator and denominator of the right-hand side are computed using Equation (4).

To illustrate, we use the two constant-load scenarios in the experimental data, where specimens were held at load levels of 3000psi and 4500psi for $t' = 4$ years and $t' = 1$ year respectively. Consider the distribution of remaining lifetime of the surviving specimens, if these constant load levels were maintained indefinitely. To obtain the survivor functions for up to 100 more years, we evaluate Equation (10) from $t_r = 0$ to 100 years for each of the MCMC samples $\theta^{(1)}, \theta^{(2)}, \ldots, \theta^{(N)}$. These are summarized in Figure 4, where the black curve shows the posterior mean of the survivor functions, and the 0.025 and 0.975 quantiles at each time point are used as the lower and upper limits of the 95% posterior bands shown in grey.

It can be seen that the distributions of T_r have very long right tails, corresponding to the strongest members of the population that can carry these load levels almost indefinitely. As such, the mean residual lifetime is not very meaningful. Instead quantities such as the time until 50% of the survivors fail, that is the median t_m such that $P[T_r > t_m \mid \xi, \eta_t] = 0.5$, may be of interest. Using Equation (10) to solve t_m for each of the MCMC samples, we obtain the following 95% posterior intervals for t_m: $(21.9, 333.5)$ years under 3000psi and $(5.2, 24.3)$ years under 4500psi. There is much more uncertainty associated with these estimates at the lower load level.

To compare these results with the fitted Canadian ADM in [26], we use 100,000 simulated failure times by solving Equation (2) and these empirical survivor functions are shown with the dashed lines in Figure 4. The residual lifetime distributions from the ADM initially are within our posterior bands, but over longer time periods have much more optimistic survival probabilities compared to our gamma process model; for example, the ADM predicts that neither of these load levels will ever cause 50% of the survivors to fail. We comment on this along with the role of the stress threshold σ_0 in the ADM in the Discussion.

7 Discussion and conclusions

In the analysis of the Hemlock experimental data we found that the effect of degradation from a constant load due to time, as modeled in the shape parameter, was not a power law t^a. This is evident by examining the plots in Figure 1. With a simple power law, the CDF would

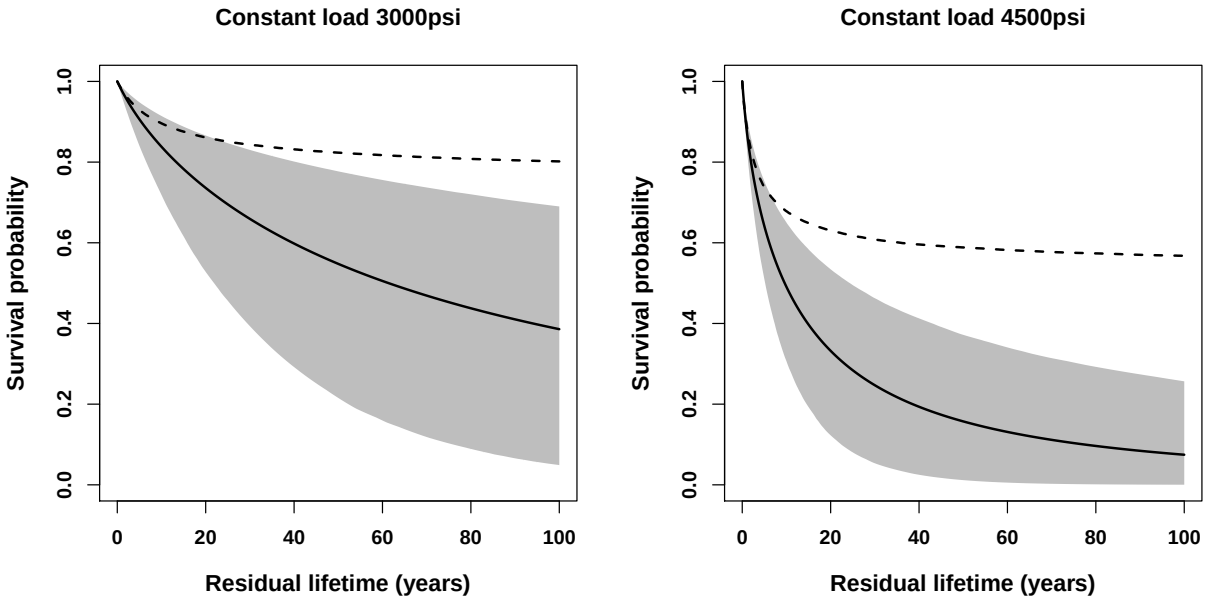

Figure 4: Residual lifetime example. Survivor functions of the remaining lifetime for specimens under a continued 3000psi constant load after surviving the 4-year test period (left panel), and for specimens under a continued 4500psi constant load after surviving the 1-year test period (right panel). The black curve shown is the posterior mean, while the grey area represents the 95% posterior interval based on the MCMC samples. The dashed lines represent the estimated survivor functions computed from the fitted Canadian ADM in [26].

be approximately linear as a function of log-time during the constant load period. Instead, the empirical CDF increases quite nonlinearly with time on the log-scale. This led us to posit adding a second power term to the model, yielding $t^a + bt^c$ with $a < c$. This form provides a reasonable fit to the data, however with wide posterior intervals for the parameters b and c. That in turn translates to the high uncertainty that we find associated with using these tests of 1 and 4 year durations to predict reliability and residual lifetime for Hemlock over much longer periods, such as 50 years. This variability could be reduced by incorporating expert knowledge into the priors for Bayesian analysis, or by using data from larger experiments, possibly of longer duration. As a future extension, it is also straightforward to use the model with a different form of $g(t)$ in Equation (6), as long as it is differentiable.

In the work by Foschi et al. [28], a crucial parameter in the Canadian ADM used for reliability analysis is the 'stress threshold' σ_0. In that model it is hypothesized that an individual piece of lumber does not accumulate damage when the load is below $\sigma_0\tau_s$, where τ_s is the strength of that piece as measured in a short-term ramp load test. That work reported an estimate for the population mean of σ_0 to be 0.533 for the Hemlock data; based on that estimate along with a population mean short-term strength of ∼6900psi, the ADM predicts that most pieces do not eventually fail under the load levels seen in the residential example of Figure 2. Similarly, the ADM predicts that a large fraction of the survivors under the constant-load test will never fail when that load is sustained (Figure 4, dashed lines). Further computational study on the ADM shows that the mean of σ_0 has much uncertainty; even values close to 0 can plausibly fit the Hemlock data when the other parameters in the model are adjusted [14]. Hence the ADM predictions that we show in this paper should be interpreted with caution, as they were based on the single set of parameter values reported in previous studies without associated confidence intervals to account for uncertainty. In another DOL study based on a separate experiment [10], the authors found no evidence of a damage threshold. It may well be that the estimate of 0.533 reflects some other, not explicitly reported prior knowledge about the behaviour of lumber, e.g. how many wood structures have survived the test of 50 or 100 years. However in the current application no information concerning that issue was available. Such information could easily be incorporated into the priors used with the gamma process approach to set more realistic constraints on the rate of degradation over longer periods.

We would further note that σ_0 as a piece-level parameter in the ADM does not have a direct relationship with our estimated damage threshold of 413psi for the Hemlock population. In the ADM, the population mean of $\sigma_0\tau_s$ is the load below which the *average* piece in the population is undamaged; however, the realization of $\sigma_0\tau_s$ cannot be assessed for any individual piece since it is unobservable. In contrast the 413psi population threshold in our

model represents the stress level below which *all* members of the population are undamaged. Nonetheless as discussed above, neither approach presents conclusive evidence of a high damage threshold in the Hemlock data, when uncertainty is considered. Specialized proof-loading tests [e.g., 29] may instead be used if estimating the damage threshold is of primary interest.

Another point of comparison between the ADM and our proposed approach lies in the number of parameters to be estimated. Fitting the Canadian ADM in particular requires estimating 10 population parameters (the five log-normal means and variances from which the random effects in Equation (2) are drawn for specific pieces of lumber), some of which do not have a clear physical interpretation. As found in [14], a number of different sets of these population parameters could lead to essentially the same likelihood, suggesting that the ADM may be over-parametrized. The resulting inflated uncertainty about the individual model parameters may lead to worsened prediction performance. Our model with four fewer parameters (six) attains a higher log-likelihood than the ADM when fit to the Hemlock data, and is favoured according to standard model selection criteria such as BIC. It is also simple to see that the parameters b and c in our model are associated with long term degradation rate and have the most uncertainty.

It can be said that the results of applying the accumulated damage modeling approach along with its predecessor, the empirical model of Wood et al. [4], have laid a foundation for incorporating long term stress effects into the calculation of design values that have stood the test of time. So why a critical review of these models at this time? The answer lies in the need for application of the methods to a new generation of forest products such as strand based wood composites [30, 19] that are also susceptible to DOL effects. Given that the new applications do not automatically inherit the record of success of the ADM, prudence suggests a re-evaluation of the approach given its limitations as described in the Introduction, one that takes full advantage of the new computational and statistical methods now available. Since engineered wood composites have much lower short-term strength variability compared to lumber, the size of the DOL effect (and its estimation) for these materials would have a more significant role in determining appropriate safety factors.

The above considerations led the authors to explore the alternative to the ADM presented in this paper and it was found to overcome many of the difficulties described above with the ADM approach. The model based on the gamma process is simpler to interpret with fewer parameters, and lends itself well to principled statistical analysis based on the likelihood function. Bayesian methods were proposed for model fitting and illustrated using data from load-duration experiments on Western Hemlock. The utility of the fitted model was demonstrated with applications involving the estimation of reliability and residual lifetime

distributions. Using the Bayesian approach, posterior intervals that quantify uncertainty in the estimates were also easily constructed. In particular, a key finding from our analysis is that the accelerated testing data on Hemlock yield highly uncertain predictions of the long term future of a piece of lumber in service, as evidenced by very wide credibility bands and posterior intervals. As these predictions are computed from the posterior samples of the parameters, strategies that reduce the variability in the posterior distributions of the parameters would lead to more reliable predictions. This can be done by incorporating appropriate expert knowledge into the priors for analysis, or using data from larger accelerated tests.

Acknowledgment

The work reported in this manuscript was partially supported by FPInnovations and a CRD grant from the Natural Sciences and Engineering Research Council of Canada. The data analysed in this paper were provided by FPInnovations. We are greatly indebted to Conroy Lum and Erol Karacabeyli from FPInnovations for their extensive advice during the conduct of the research reported herein.

References

[1] E. Karacabeyli and L. A. Soltis, "State of the art report on duration of load research for lumber in north america," in *Proceedings of the 1991 International Timber Engineering Conference. London, United Kingdom*, 1991.

[2] D. V. Rosowsky and W. M. Bulleit, "Another look at load duration effects in wood," *Journal of Structural Engineering*, vol. 128, no. 6, pp. 824–828, 2002.

[3] H. Haupt, *General theory of bridge construction*. New York: Appleton, 1867.

[4] L. W. Wood *et al.*, *Relation of strength of wood to duration of load*. Madison, Wis.: US Dept. of Agriculture, Forest Service, Forest Products Laboratory, 1960.

[5] J. Barrett and R. Foschi, "Duration of load and probability of failure in wood. part i. modelling creep rupture," *Canadian Journal of Civil Engineering*, vol. 5, no. 4, pp. 505–514, 1978.

[6] ——, "Duration of load and probability of failure in wood. part ii. constant, ramp, and cyclic loadings," *Canadian Journal of Civil Engineering*, vol. 5, no. 4, pp. 515–532, 1978.

[7] C. C. Gerhards, "Time-related effects on wood strength: A linear cumulative damage theory." *Wood science*, vol. 11, pp. 139–144, 1979.

[8] R. O. Foschi, "Reliability of wood structural systems," *Journal of Structural Engineering*, vol. 110, no. 12, pp. 2995–3013, 1984.

[9] B. Ellingwood and D. Rosowsky, "Duration of load effects in lrfd for wood construction," *Journal of Structural Engineering*, vol. 117, no. 2, pp. 584–599, 1991.

[10] P. Hoffmeyer and J. D. Sørensen, "Duration of load revisited," *Wood Science and Technology*, vol. 41, no. 8, pp. 687–711, 2007.

[11] Y. Zhai, "Dynamic duration of load models," Master's thesis, University of British Columbia, Department of Statistics, 2011.

[12] Y. Zhai, C. Pirvu, N. Heckman, C. Lum, L. Wu, and J. V. Zidek, "A review of dynamic duration of load models for lumber strength," TR 270, Department of Statistics, University of British Columbia, Tech. Rep., 2012.

[13] S. W. Wong and J. V. Zidek, "Dimensional and statistical foundations for accumulated damage models," *Wood Science and Technology*, vol. 52, no. 1, pp. 45–65, 2018.

[14] C.-H. Yang, J. V. Zidek, and S. W. Wong, "Bayesian analysis of accumulated damage models in lumber reliability," *Technometrics*, 2018.

[15] J. Lawless and M. Crowder, "Covariates and random effects in a gamma process model with application to degradation and failure," *Lifetime Data Analysis*, vol. 10, no. 3, pp. 213–227, 2004.

[16] J. Van Noortwijk, "A survey of the application of gamma processes in maintenance," *Reliability Engineering & System Safety*, vol. 94, no. 1, pp. 2–21, 2009.

[17] J. Van Noortwijk, M. Kallen, and M. Pandey, "Gamma processes for time-dependent reliability of structures," *Advances in safety and reliability, proceedings of ESREL*, pp. 1457–1464, 2005.

[18] M. Guida, F. Postiglione, and G. Pulcini, "A time-discrete extended gamma process for time-dependent degradation phenomena," *Reliability Engineering & System Safety*, vol. 105, pp. 73–79, 2012.

[19] J. B. Wang, F. Lam, and R. O. Foschi, "Duration-of-load and creep effects in strand-based wood composite: experimental research," *Wood science and technology*, vol. 46, no. 1-3, pp. 361–373, 2012.

[20] C. Paroissin and A. Salami, "Failure time of non homogeneous gamma process," *Communications in Statistics-Theory and Methods*, vol. 43, no. 15, pp. 3148–3161, 2014.

[21] R. O. Foschi and J. D. Barrett, "Load-duration effects in western hemlock lumber," *Journal of the Structural Division*, vol. 108, pp. 1494–1510., 1982.

[22] ASTM, "Standard test methods for mechanical properties of lumber and wood-base structural material," 1991.

[23] W. K. Hastings, "Monte carlo sampling methods using markov chains and their applications," *Biometrika*, vol. 57, no. 1, pp. 97–109, 1970.

[24] J. S. Liu, *Monte Carlo strategies in scientific computing*. Springer Science & Business Media, 2008.

[25] R. H. Swendsen and J.-S. Wang, "Replica monte carlo simulation of spin-glasses," *Physical Review Letters*, vol. 57, no. 21, p. 2607, 1986.

[26] F. Z. Yao and R. O. Foschi, "Duration of load in wood: Canadian results and implementation in reliability-based design," *Canadian Journal of Civil Engineering*, vol. 20, no. 3, pp. 358–365, 1993.

[27] G. Schwarz *et al.*, "Estimating the dimension of a model," *The annals of statistics*, vol. 6, no. 2, pp. 461–464, 1978.

[28] R. O. Foschi, B. Folz, and F. Yao, *Reliability-based design of wood structures*. Dept. of Civil Engineering, University of British Columbia, 1989, no. 34.

[29] F. Woeste, D. Green, K. Tarbell, and L. Marin, "Proof loading to assure lumber strength," *Wood and fiber science*, vol. 19, no. 3, pp. 283–297, 2007.

[30] J. B. Wang, R. O. Foschi, and F. Lam, "Duration-of-load and creep effects in strand-based wood composite: a creep-rupture model," *Wood science and technology*, vol. 46, no. 1-3, pp. 375–391, 2012.